Supporting Information

A study of the complex interaction between poly allylamine hydrochloride and negatively charged poly(N-isopropylacrylamide-co-methacrylic acid) microgels

Juan M. Giussi,[1*] Marta Martínez Moro,[2] Agustín Iborra,[1] M. Lorena Cortez,[1] Desiré Di Silvio,[2] Irantzu Llarena Conde,[2] Gabriel S. Longo,[1] Omar Azzaroni,[1] and Sergio Moya[2*]

[1] Instituto de Investigaciones Fisicoquímicas Teoricas y Aplicadas (INIFTA) – Departamento de Química – Facultad de Ciencias Exactas - Universidad Nacional de La Plata – CONICET, 1900 La Plata – Argentina.

[2] Soft Matter Nanotechnology Group, CIC BiomaGUNE, Paseo Miramon 182, 20014, San Sebastian, España

Microgel synthesis and characterization

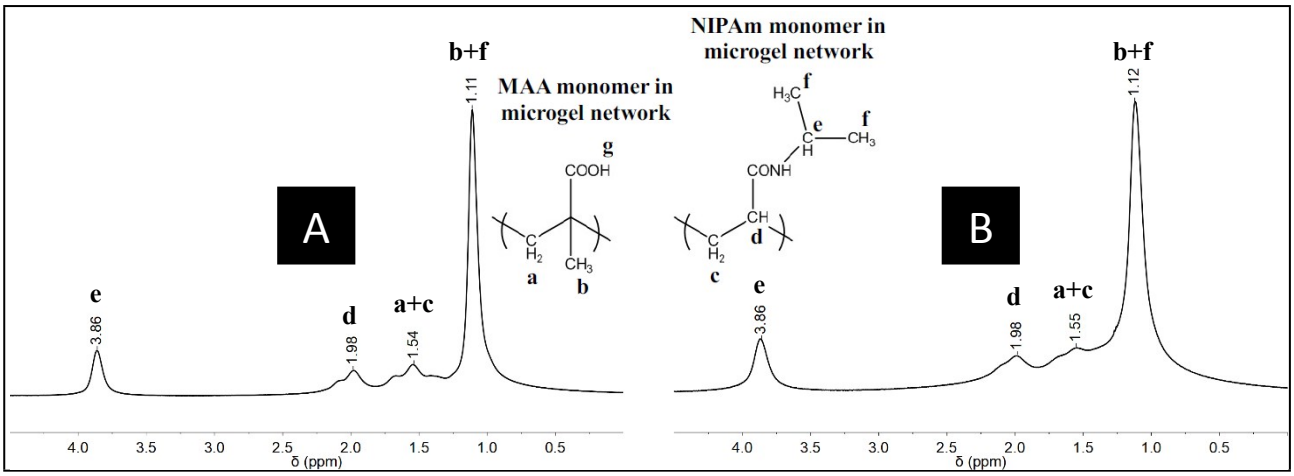

Figure S1. ^{1}H NMR spectrum with assignments for a P(NIPAm-*co*-MAA) microgel, a) statistical and b) core-shell.

The final composition of the microgels were estimated from ^{1}H NMR spectrum: 88% NIPAm and 12% MMA (0.88:0.12) for the conventional (statistical) particle and 81% NIPAm and 19% MMA (0.81:0.19) for the core shell structure.

Dynamic light scattering (DLS) measurements

The size and size distribution of PNIPAm-based microgels were determined by dynamic light scattering (DLS) as a function of temperature using a Zetasizer Nano-ZS90 (MalvernInstruments Ltd.). Table S1 shows the size and PDI values obtained with 1 mg/ml microgel dispersions in 5 mM KCl exposed to increasing amounts of PAH of different molecular weights (15, 50, and 140 kDa) at 20 and 40°C.

Table S1. Size and PDI values obtained by dynamic light scattering at 20 and 40°C for P(NIPAm-*co*-MAA) microgels with increasing amount of PAH of 15 kDa, 50 kDa and 140 kDa.

PAH → MW	15kDa				50kDa				140kDa			
↓	20°C		40°C		20°C		40°C		20°C		40°C	
Amount (%)	D_H	PDI	D_H	PDI	D_H	PDI	D_H	PDI	D_H	PDI	D_H	PDI
0	1181	0,298	424,2	0,034	1181	0,298	424,2	0,034	1181	0,298	424,2	0,034
5	865,9	0,152	494,1	0,061	3370	1	1917	0,329	4007	0,309	1956	0,27
10	805,1	0,095	407,7	0,029	1044	0,335	728,9	0,262	1488	0,243	1378	0,104
20	834,8	0,095	473,3	0,332	851,9	0,157	744,6	0,045	1340	0,303	1367	0,302
40	976,5	0,228	517	0,238	912,5	0,178	856,4	0,017	1701	0,198	1161	0,242
80	956,2	0,151	566,5	0,012	1421	0,238	891,1	0,065	Precipitation			
120	1129	0,211	691,9	0,096	Precipitation							
160	1284	0,321	652,9	0,062								

Molecular Theory: PAH adsorption to a p(NIPAm-co-MAA) film

To study the equilibrium adsorption of PAH to hydrogel films of grafted cross-linked P(NIPAm-*co*-MAA) chains, we have applied molecular theory with explicit description of all chemical species that compose the system. The protonation state of each of the different titratable units of MAA is not assumed but predicted as a result of the local interplay between the free energy cost of protonation/deprotonation, the entropic loss of molecular confinement, the conformational degrees of freedom of the network and the PAH adsorbate, and electrostatic and steric interactions. To this end, we write a general free energy that includes all of these contributions. This molecular theory was originally developed to study adsorption of histidine peptides to grafted polyacid networks,[1] and has been recently extended to investigate protein protonation upon adsorption to such hydrogel films.[2] This method is based on an extension of the works by Nap et al.[3] and Gong et al.[4] to study the behaviour of grafted weak polyelectrolyte layers. Here, we will only outline the theoretical method and highlight the differences with previous studies, in particular the temperature-response of PNIPAm; a full description of the theory can be found in recent work.[5]

Our system is composed of an aqueous solution in contact with a network of cross-linked P(NIPAm-*co*-MAA) that is chemically grafted to a planar surface of area A. The coordinate z

measures the distance from the supporting surface, which is placed at $z = 0$. The solution contains water, hydronium ions, hydroxide ions, and salt (KCl) dissociated into potassium and chloride ions. This solution can also contain PAH chains.

The Helmholtz free energy of this system can be expressed as:

$$F = -TS_{cnf,nw} + F_{chm,nw} - TS_{mix} - TS_{tr,PAH} - TS_{cnf,PAH} + U_{st} + U_{elect} + U_{vdw} \quad \text{(S1)}$$

where T is the temperature. The first term in the right-hand side of this equation is the conformational entropy of the network ($S_{cnf,nw}$) that arises from the many possible spatial distributions of NIPAm and MAA segments (conformations). The second term is the chemical free energy of the network ($F_{chm,nw}$) that accounts for the acid-base equilibrium of MAA units. The next term accounts for the translational (mixing) entropy and self-energy of the free species (S_{mix}), except PAH chains. Similarly, $S_{tr,PAH}$ describes the translation and self-energy of these polymer chains. In addition to their rotational freedom, PAH chains can assume different molecular conformations (having different spatial distributions of segments, relative to the center of mass of the molecule); $S_{cnf,PAH}$ accounts for this entropic contribution to the free energy. The second line in Eq. (S1) includes steric (excluded volume) repulsions (U_{st}) and electrostatic interactions (U_{elect}). Lastly, the van der Waals attractions account for NIPAm response to temperature changes. To model this contribution, we follow the work of Afroze et al.[6]

$$\beta\frac{U_{vdw}}{A} = \int_0^\infty dz \frac{\chi\left(T, \langle\phi_{NIPAm}(z)\rangle\right)}{v_w}\phi_w(z)\langle\phi_{NIPAm}(z)\rangle \quad \text{(S2)}$$

where $\phi_w(z)$ and $\langle\phi_{NIPAm}(z)\rangle$ are the local volume fractions of water and NIPAm segments, respectively; v_w is the volume of a water molecule and $\beta = \frac{1}{k_B T}$ with k_B the Boltzmann constant; angle brackets indicate ensemble average over network conformations. The interaction parameter is

$$\chi\left(T, \langle\phi_{NIPAm}(z)\rangle\right) = g_0(T) + g_1(T)\,\langle\phi_{NIPAm}(z)\rangle + g_2(T)\,\langle\phi_{NIPAm}(z)\rangle^2 \quad \text{(S3)}$$

with

$$g_k(T) = g_{k0} + \frac{g_{k1}}{T} + g_{k2}T \quad \text{(S4)}$$

where the coefficients are[6] $g_{00} = -12.947$, $g_{02} = 0.044959$, $g_{10} = 17.920$, $g_{12} = -0.056944$, $g_{20} = 14.814$, $g_{22} = -0.051419$ and $g_{k1} \equiv 0$.

As seen with U_{vdw}, all the contributions to the free energy can be explicitly written in terms of a few functions: (i) the local densities (or volume fractions) of all free species, (ii) the local density of different molecular conformations of PAH, (iii) the probability distribution of network conformation, which provides $\langle \phi_{NIPAm}(z) \rangle$ and the local volume fraction of MAA segments $\langle \phi_{MAA}(z) \rangle$, (iv) the local degrees of protonation of MAA, (v) the local electrostatic potential. The next step is the optimization of the free energy with respect to each of these functions. Such procedure allows for expressing functions (i) to (iv) in terms of only two position-dependent interaction potentials, the local osmotic pressure and the electrostatic potential, and the local volume fraction of NIPAm segments.

These local functions can be numerically calculated through iteratively solving both the Poisson equation and the incompressibility constraint imposed to the fluid. This last restriction assures that, at each position, the available volume is fully occupied by some of the chemical species. After these interaction potentials and the local volume fraction of NIPAm are determined the free energy of the system is known; any thermodynamic quantity of interest can be derived from the free energy. The local functions that compose the free energy are known as well, which allows for the calculation of different local and average quantities

In order to apply this theory, a molecular model must be defined to describe each chemical species. The P(NIPAm-*co*-MAA) network is composed of cross-linked 50-segment long polymer chains, where each segment is a coarse-grained representation of either a NIPAm or a MAA unit, having 0.5nm segment length and volume 0.11nm^3. Most of these chains connect two cross-linking segments, except those top-most chains, which have their solution-side ends free, and some chains that are connected by one of their ends to a surface-grafted segment. Cross-linking units have coordination four and the structure has diamond-like topology.[7–10] To generate network conformations, we have performed MD simulations using GROMACS 5.1.2,[11–13] where the network is a periodic molecule composed of 30 cross-linking segments, 2 grafting points, and 64 chains with a total of 2560 NIPAm and 640 MAA units (3200 segments with a 80:20 NIPAm:MAA ratio). The supporting surface in the MD simulation box has a 33nm^2 area; periodic boundary conditions are

imposed in both the x and y directions. The force field used in this MD simulations has been well described in other works.[7,9,14,15]

Poly(allylamine) molecules are 50-segment long chains, where each segment is a coarse-grained representation of an allylamine unit, having 0.5nm segment length and volume 0.11nm^3. A large number (10^5) of molecular conformations of a PAH chain were generated using a rotational isomeric state model,[16] where each segment can randomly assume one of three isoenergetic orientations. Each of these conformations is rotated 12 times using random Euler angles and translated throughout the system.

Other inputs of our molecular model are the volume (and charge) of the rest of the free species: for water molecules, hydronium and hydroxyde ions we use 0.03nm^3, while the volume of salt ions is 0.033 nm^3. In order to numerically solve the equations resulting from the molecular theory, the Poisson equation and the incompressibility constraint, space is discretized into 0.5 nm-thick layers parallel to the supporting surface (the x-y plane). The system is assumed to be isotropic in the x and y directions. The aqueous medium has dielectric constant $\varepsilon_w\varepsilon_0$, where ε_w = 78.5 is the relative dielectric constant of water at room temperature, and ε_0 is the permittivity of vacuum. For the self-dissociation of water, we use pK_w = 14, while for the acid dissociation of MAA we use pK_a=4.65.

Confocal Microscopy and Flow Cytometry Determinations

Confocal microscopy imaging was performed with Confocal Microscope ZeissLSM 880 (Carl Zeiss Gmbh). Acquisition and analysis are controlled by Zen black software. Excitation wavelength was 488nm argon laser and emission collected using GaASP detector. coupled with transmission, T-PTM. The objective used was 100x EC Plan-Neofluar(oil, 1.3 NA) objective. The kinetic experiments were carried out acquiring 1024x1024 pixels frames, 10x digital zoom and 120 time series with 1.2 s frame rate. Samples were stabilized for 10 minutes at different temperatures before time series acquisition using temperature-controlled insert in the microscope stage. FACS experiment was performed with BD FACSCanto II instrument. PE channel (585/42 nm filter with a 556 nm long pass filter) was used to study labelled PAH uptake inside the microgel. BD™ CS&T Beads were run before the experiment to ensure the correct performance of the instrument. To determine the microgel population non labelled microgel was used by means of forward (FSC) and side scatter (SSC) characteristics. Microgel unlabeled and labelled with the maximum percentage of PAH were employed to fix the PE-A voltage. 10 000 events were acquired for each sample. FlowJo 7.5 software was used to analyze the data.

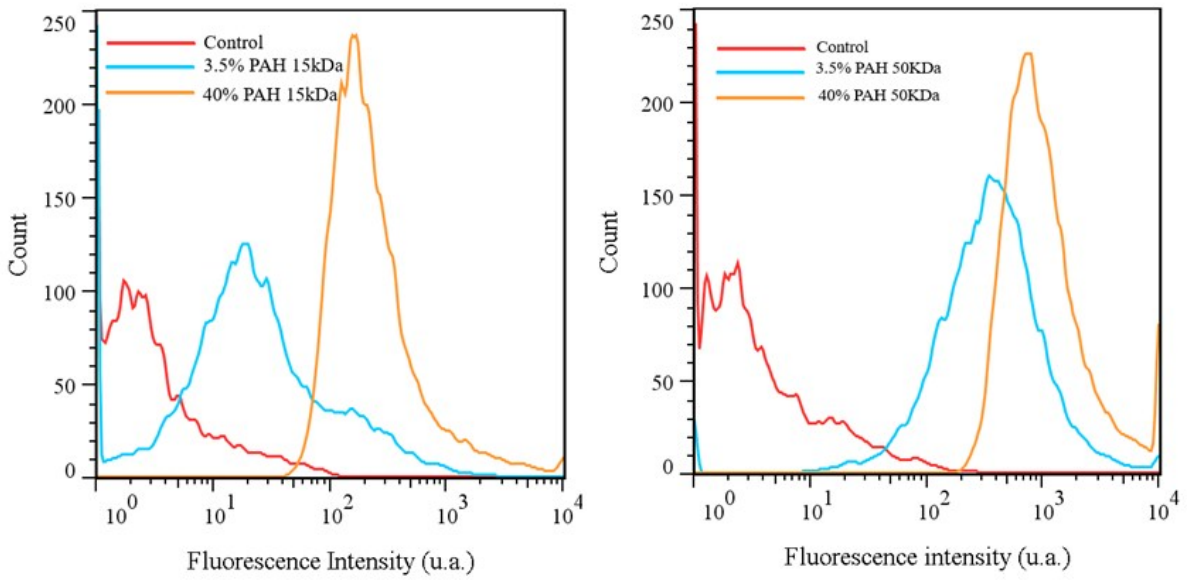

Figure S2: Fluorescence intensity vs. particle number distribution: a) PAH 15kDa and b) PAH 50kDa.

References

1 G. S. Longo, M. Olvera de la Cruz and I. Szleifer, *Langmuir*, 2014, **30**, 15335–15344.
2 G. S. Longo, M. Olvera de la Cruz and I. Szleifer, *Soft Matter*, 2016, **12**, 8359–8366.
3 R. Nap, P. Gong and I. Szleifer, *J. Polym. Sci. Part B Polym. Phys.*, 2006, **44**, 2638–2662.
4 P. Gong, J. Genzer and I. Szleifer, *Phys. Rev. Lett.*, 2007, **98**, 18302.
5 A. Hagemann, J. M. Giussi and G. S. Longo, *The use of pH gradients in responsive polymer hydrogels for the separation and localization of proteins from binary mixtures*, .
6 F. Afroze, E. Nies and H. Berghmans, *J. Mol. Struct.*, 2000, **554**, 55–68.
7 B. A. Mann, C. Holm and K. Kremer, *J. Chem. Phys.*, 2005, **122**, 154903.
8 M. Quesada-Pérez, J. A. Maroto-Centeno and A. Martín-Molina, *Macromolecules*, 2012, **45**, 8872–8879.
9 P. Košovan, T. Richter and C. Holm, *Macromolecules*, 2015, **48**, 7698–7708.
10 C. Hofzumahaus, P. Hebbeker and S. Schneider, *Soft Matter*, 2018, **14**, 4087–4100.
11 H. J. C. Berendsen, D. van der Spoel and R. van Drunen, *Comput. Phys. Commun.*, 1995, **91**, 43–56.
12 D. van der Spoel, E. Lindahl, B. Hess, G. Groenhof, A. E. Mark and H. J. C. Berendsen, *J. Comput. Chem.*, 2005, **26**, 1701–1718.
13 M. J. Abraham, T. Murtola, R. Schulz, S. Páll, J. C. Smith, B. Hess and E. Lindahl, *SoftwareX*, 2015, **1–2**, 19–25.
14 K. Kremer and G. S. Grest, *J. Chem. Phys.*, 1990, **92**, 5057.
15 G. S. Longo, M. Olvera De La Cruz and I. Szleifer, *Macromolecules*, 2011, **44**, 147–158.
16 P. J. Flory, *Statistical Mechanics of Chain Molecules*, Hanser, 1989.